

Quantum Gravity in the Lab: Teleportation by Size and Traversable Wormholes

Adam R. Brown,^{1,2} Hrant Gharibyan,^{2,3} Stefan Leichenauer,¹ Henry W. Lin,^{1,4} Sepehr Nezami,^{1,2} Grant Salton,^{3,2} Leonard Susskind,^{1,2} Brian Swingle,⁵ and Michael Walter⁶

¹*Google, Mountain View, CA 94043, USA*

²*Department of Physics, Stanford University, Stanford, CA 94305, USA*

³*Institute for Quantum Information and Matter, Caltech, Pasadena CA 91125, USA*

⁴*Physics Department, Princeton University, Princeton, NJ 08540, USA*

⁵*Condensed Matter Theory Center, Joint Center for Quantum Information and Computer Science, Maryland Center for Fundamental Physics, and Department of Physics, University of Maryland, College Park, MD 20742, USA*

⁶*Korteweg-de Vries Institute for Mathematics,*

Institute for Theoretical Physics, Institute for Logic,

Language and Computation & QuSoft, University of Amsterdam, The Netherlands

With the long-term goal of studying quantum gravity in the lab, we propose holographic teleportation protocols that can be readily executed in table-top experiments. These protocols exhibit similar behavior to that seen in the recent traversable wormhole constructions of [1, 2]: information that is scrambled into one half of an entangled system will, following a weak coupling between the two halves, unscramble into the other half. We introduce the concept of *teleportation by size* to capture how the physics of operator-size growth naturally leads to information transmission. The transmission of a signal *through* a semi-classical holographic wormhole corresponds to a rather special property of the operator-size distribution we call *size winding*. For more general setups (which may not have a clean emergent geometry), we argue that imperfect size winding is a generalization of the traversable wormhole phenomenon. For example, a form of signalling continues to function at high temperature and at large times for generic chaotic systems, even though it does *not* correspond to a signal going through a geometrical wormhole, but rather to an interference effect involving macroscopically different emergent geometries. Finally, we outline implementations feasible with current technology in two experimental platforms: Rydberg atom arrays and trapped ions.

CONTENTS

I. Introduction	2
A. The Quantum Circuit	3
B. Quantum Circuits as Wormholes	4
C. Overview	5
II. Teleportation by Size	6
A. Size Winding	6
B. State Transfer by Size-Dependent Phase	8
C. General Bounds on the Fidelity	9
III. The Holographic Interpretation	10
A. Size and momentum	11
B. Superpositions of Geometries at Large Times	12
C. Wormhole Tomography and Other Future Directions	12
IV. Experimental Realization	13
A. Rydberg atom arrays	14
B. Trapped ions	16
C. Closing remarks	16
Acknowledgements	16
References	17

I. INTRODUCTION

In the quest to understand the quantum nature of spacetime and gravity, a key difficulty is the lack of contact with experiment. Since gravity is so weak, directly probing quantum gravity means going to experimentally infeasible energy scales. However, a consequence of the holographic principle [3, 4] and its concrete realization in the AdS/CFT correspondence [5–7] (see also [8]) is that non-gravitational systems with sufficient entanglement may exhibit phenomena characteristic of quantum gravity. This suggests that we may be able to use table-top physics experiments to probe quantum gravity indirectly. Indeed, the technology for the control of complex quantum many-body systems is advancing rapidly, and we appear to be at the dawn of a new era in physics—the study of quantum gravity in the lab.

The purpose of this paper is to discuss one way in which quantum gravity can make contact with experiment. We will focus on a surprising communication phenomenon. We will examine a particular entangled state—one that could actually be made in an atomic physics lab—and consider the fate of a message inserted into the system in a certain way. Since the system is chaotic, the message is soon dissolved amongst the constituent parts of the system. The surprise is what happens next. After a period in which the message seems thoroughly scrambled with the rest of the state, the message then abruptly unscrambles, and recoheres at a point far away from where it was originally inserted. The signal has unexpectedly refocused, without it being at all obvious what it was that acted as the lens.

One way to describe this phenomenon is just to brute-force use the Schrodinger equation. But what makes this phenomenon so intriguing is that it has a much simpler explanation, albeit a simple explanation that arises from an unexpected direction [1]. If we imagine the initial entangled quantum state consists of two entangled black holes, then there is a natural explanation for why the message reappears—it travelled through a wormhole connecting the two black holes! This is a phenomenon that one could prospectively realize in the lab that has as its most compact explanation a story involving emergent spacetime dimensions.

An analogy may be helpful. Consider two people having a conversation, or as a physicist might describe it “exchanging information using sound waves”. From the point of view of molecular dynamics, it is remarkable that they can communicate at all. The room might contain 10^{27} or more molecules with a given molecule experiencing a collision every 10^{-10} s or so. In such a system, it is effectively impossible to follow the complete dynamics: the butterfly effect implies that a computer would need roughly 10^{37} additional bits of precision every time it propagated the full state of the system for one more second. Communication is possible despite the chaos because the system nevertheless possesses emergent collective modes—sound waves—which behave in an orderly fashion.

When quantum effects are important, complex patterns of entanglement can give rise to qualitatively new kinds of emergent collective phenomena. One extreme example of this kind of emergence is precisely the holographic generation of spacetime and gravity from entanglement, complexity, and chaos. In such situations, new physical structures become possible, including wormholes which connect distant regions of spacetime. And like the physics of sound in the chaotic atmosphere of the room, the physics of these wormholes points the way to a general class of quantum communication procedures which would otherwise appear utterly mysterious. The experimental study of such situations therefore offers a path toward a deeper understanding of quantum gravity. By probing stringy corrections to the gravitational description, a sophisticated experiment of this type could even provide an experimental test of string theory.

A. The Quantum Circuit

In this paper, we will consider the quantum circuits shown in Fig. 1. These circuits, which as we will see in Sec. IV may be readily created in a laboratory, exhibit the strange recoherence phenomenon we have described.

The circuits act on a $2n$ -qubit state. The qubits are divided into n qubits on the left, and n qubits on the right, subject to ‘opposite’ Hamiltonians H and H^T respectively, which are assumed to be scrambling [9, 10]. The left and right qubits are initially entangled in the “thermofield double” (TFD) state,

$$|\text{TFD}\rangle = \frac{1}{\sqrt{\text{tr } e^{-\beta H}}} \sum_{j \in \text{energy levels}} e^{-(1/2)\beta E_j} \overline{|E_j\rangle}_L \otimes |E_j\rangle_R, \quad (1)$$

where β is the inverse temperature, $H |E_j\rangle = E_j |E_j\rangle$, and the bar indicates complex conjugation. We then further partition the systems, labelling $m \ll n$ of the qubits on each side the ‘message’ qubits, and the remaining $n - m$ the ‘carrier’ qubits.

Step one is to bury the message in the left system. First we evolve all the left qubits ‘backward in time’ by acting with the inverse of the time-evolution operator, e^{iHt_L} . Next we insert the message into the message subsystem of the left qubits. Figure 1(a) shows one way to do this—we just throw the existing m qubits away, and replace them with our m -qubit message Ψ_{in} . Figure 1(b) shows another way to do this—keep the m qubits around but act on them with an operator O . Next we

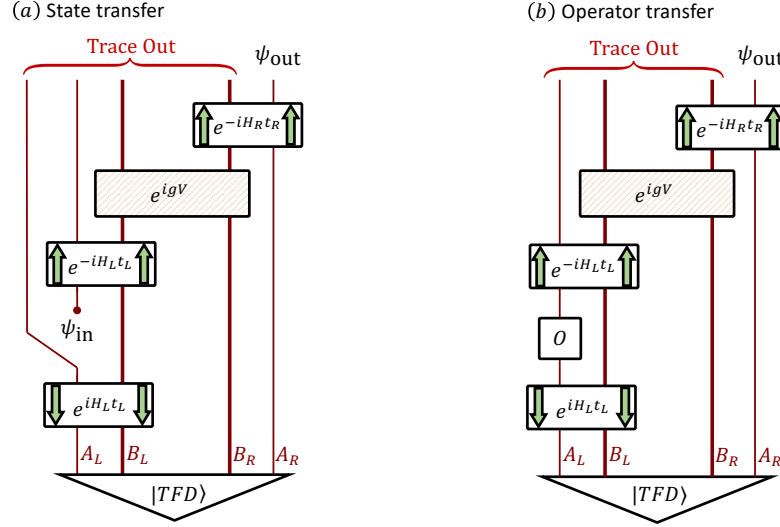


Figure 1. The circuits considered in this paper, with $H_L = H_R^T$. Downward arrows indicate acting with the inverse of the time-evolution operator. In both protocols, the goal is to transmit information from the left to the right. The **(a) state transfer** protocol calls for us to discard the left message qubits (A_L) and replace them with our message Ψ_{in} . The output state on the right then defines a channel applied to the input state. The **(b) operator transfer** protocol calls for the operator O to be applied to A_L . Based on the choice of operator, the output state on the right is modified, similar to a perturbation-response experiment.

evolve the left system ‘forward in time’ using e^{-iHt_L} . This forward evolution rapidly scrambles the message amongst the n left qubits.

The next step is to couple the left and right qubits by acting with

$$\exp(igV), \quad \text{where } V = \frac{1}{n-m} \sum_{i \in \text{carrier qubits}} Z_i^L Z_i^R, \quad (2)$$

where $Z_i := (\sigma_z)_i$. This couples each of the left carrier qubits to its mirror image on the right. Finally, we evolve all n of the right qubits ‘forward in time’ using e^{-iHt_R} .

It is at this stage that a surprising phenomenon occurs for $t_R \sim t_L$. In the case of state transfer, Figure 1(a), the message, so carefully buried on the left, may reappear on the right. In the case of operator transfer, Figure 1(b), the action of the operator, so carefully hidden on the left, may become manifest again on the right. The surprise is not that it is information-theoretically possible to recover the message on the right—after all, we coupled the left and right systems with e^{igV} . Instead, the surprise is one of complexity rather than information theory—with the right parameters, we don’t need to decode anything, the message just presents itself refocused on the right. It is not at all obvious how the message made it, and the most surprising fact of all is that the simplest explanation lies in the physics of black holes.

B. Quantum Circuits as Wormholes

The AdS/CFT duality is a correspondence between gravitational systems in Anti-de Sitter (AdS) space-times and non-gravitational quantum conformal field theories (CFT). A CFT in the thermofield-double state of Eq. (1) would be dual to the two-sided eternal black hole shown in

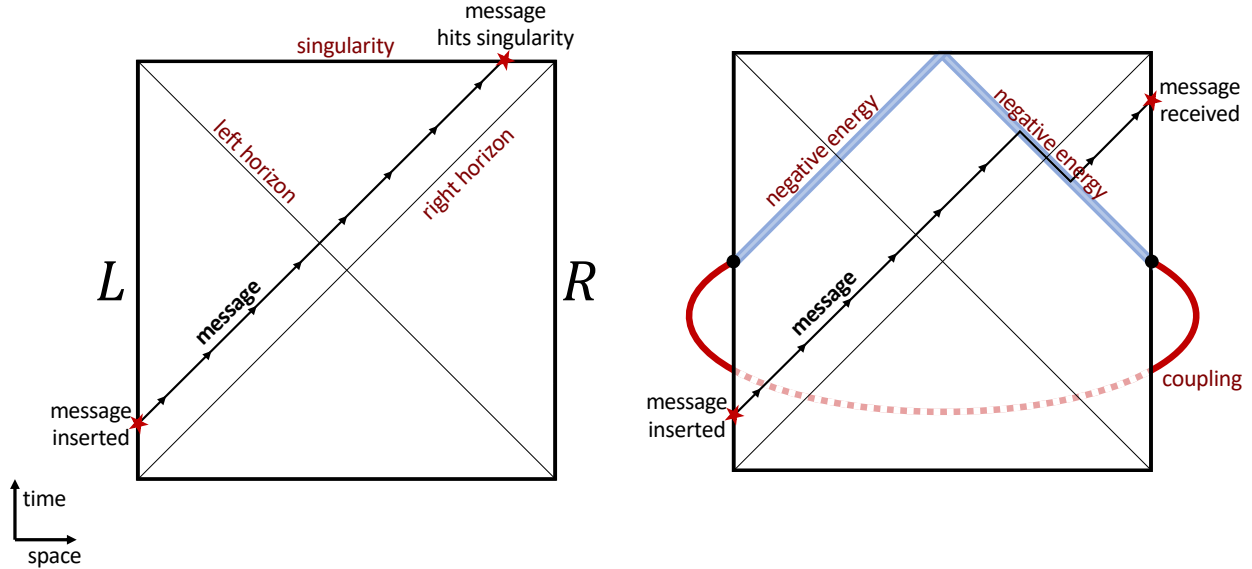


Figure 2. Penrose diagram of wormholes. **Left:** Without the coupling, a message or particle inserted at early times on the left passes through the left horizon, and hits the singularity (the top line of the diagram). **Right:** In the presence of the left-right coupling, the message hits the negative energy shockwave (the thick blue line) created by the coupling. The effect of the collision is to rescue the message from behind the right horizon.

Fig. 2. Such black holes are called ‘two-sided’ because they feature two asymptotic $r = \infty$ regions connected by a wormhole. A pair of observers who jump in from each side may meet before they hit the singularity, but the wormhole is not “traversable” since it is not possible to send a signal from the left asymptotic region all the way to the right asymptotic region.

However, in [1] it was shown how to render such wormholes traversable. A suitably chosen direct coupling between the two sides, which ordinarily do not interact, produces a negative energy shockwave. Negative energy shockwaves impart a time advance to whatever they encounter, and so can rescue a signal that would otherwise be lost to the singularity (Fig. 2).

It is this gravitational scattering process that the circuit in Figure 1 mimics, although the interpretation of the process as traversing a wormhole is *not* valid in general (see Sec. III). From the gravity perspective, the thermofield double state is used because it exhibits strong left-right correlations (due to the wormhole) that permit negative energy injection. The backward/forward time evolution on the left corresponds to injecting a message in the past on the left. The left-right coupling is the analog of the negative energy shockwave. Finally, the subsequent forward evolution on the right corresponds to allowing the message to travel out to the right boundary where it emerges unscrambled.

C. Overview

In Sec. II, we study the circuit of Fig. 1 using quantum mechanics, without assuming a holographic dual. We introduce the notion of *teleportation by size*¹ as an information theoretic umbrella

¹ A note on terminology. ‘Quantum teleportation’ [11] refers to using pre-existing entanglement together with classical communication to send a quantum message. If we can do the state-transfer protocol, then we can certainly teleport in the following way [2]. Instead of acting with e^{igV} , one can simply measure all the left carrier qubits in the z -basis, send the classical measurement outcomes $z_i \in \{-1, 1\}$ over to the right-hand side, and act by $e^{ig \sum_i z_i Z_i^R / (n-m)}$ on the right carrier qubits. This protocol would teleport the message qubits to the right system. It works because the V coupling is *classical*, i.e., it acts on the left system through a set of commuting operators.

notion that captures the different ways that information can be transmitted using a coupling that is sensitive to operator sizes. We first explain the key mechanism of the operator transfer protocol based on a property called *size winding* of the operator-size distribution. Next we consider the state transfer protocol. Here we give general formulas for the fidelity of teleportation and show that, under the general assumption of chaos, teleportation can be achieved with high fidelity for messages that are inserted at very large times, $t_L \sim t_R \rightarrow \infty$.

In Sec. III we explain how, in the context of a system with a clean holographic dual, size winding has a direct interpretation in terms of momentum wavefunctions of bulk particles in some appropriate time regime. However, even in the holographic setting, teleportation by size does not always correspond to particles traversing semiclassical geometrical wormholes, but rather the quantum interference of two distinct classical geometries. This includes the transmission of signals sent at very large early times, as observed in [2, 12].

In Sec. IV we discuss concrete experimental realizations of teleportation by size. Unlike the field theories of AdS/CFT, systems that can be realized in an atomic physics lab all have only a finite number of degrees of freedom. We will show that having an infinite number of degrees of freedom is not necessary for the transmission of information, and indeed we will explicitly describe a modest quantum system that manifests the phenomenon.

A detailed analysis of many of the results presented here will be provided in [13]. Other studies of information transfer through traversable wormholes, and related notions, include [14, 15].

II. TELEPORTATION BY SIZE

We base most of our analysis in this paper on size distributions and operator growth, notions heavily studied in connection to holography [16–18] and many-body physics [19–21]—hence the term *teleportation by size*. In Sec. II A, we introduce a property of size distributions, called *size winding*. Size winding gives a clean mechanism for operator transfer that abstracts the way geometrical wormholes work at the level of the boundary theory (we discuss the latter in Sec. III below). In Secs. II B and II C we discuss the state transfer protocol. We will see that state transfer can be done for very generic chaotic quantum systems—even at infinite temperature—and give general bounds on the fidelity.

A. Size Winding

Consider an observable O and its transpose (in the computational basis) O^T acting at time $-t$ on the left Hilbert space. Using the definition of the TFD state, this can be expressed as:

$$\frac{1}{2^{n/2}} O_L^T(-t) |\text{TFD}\rangle_{LR} = (\rho_\beta^{1/2})_R O_R(t) |\phi^+\rangle_{LR}, \quad (3)$$

where $O(t) = e^{iHt} O e^{-iHt}$, $\rho_\beta = e^{-\beta H} (\text{tr} e^{-\beta H})^{-1}$ is the thermal state, and $|\phi^+\rangle$ denotes the maximally entangled state. The application of $O_L^T(-t)$ should be contrasted with the action of $O_R(t)$ directly on the thermofield double state:

$$\frac{1}{2^{n/2}} O_R(t) |\text{TFD}\rangle_{LR} = O_R(t) (\rho_\beta^{1/2})_R |\phi^+\rangle_{LR}. \quad (4)$$

Importantly, the only difference between Eqs. (3) and (4) is the order of insertion of $\rho_\beta^{1/2}$ and $O(t)$, and $\rho_\beta^{1/2} O(t) = (O(t) \rho_\beta^{1/2})^\dagger$. Now, expand the operator $\rho_\beta^{1/2} O(t)$ in the Pauli basis as

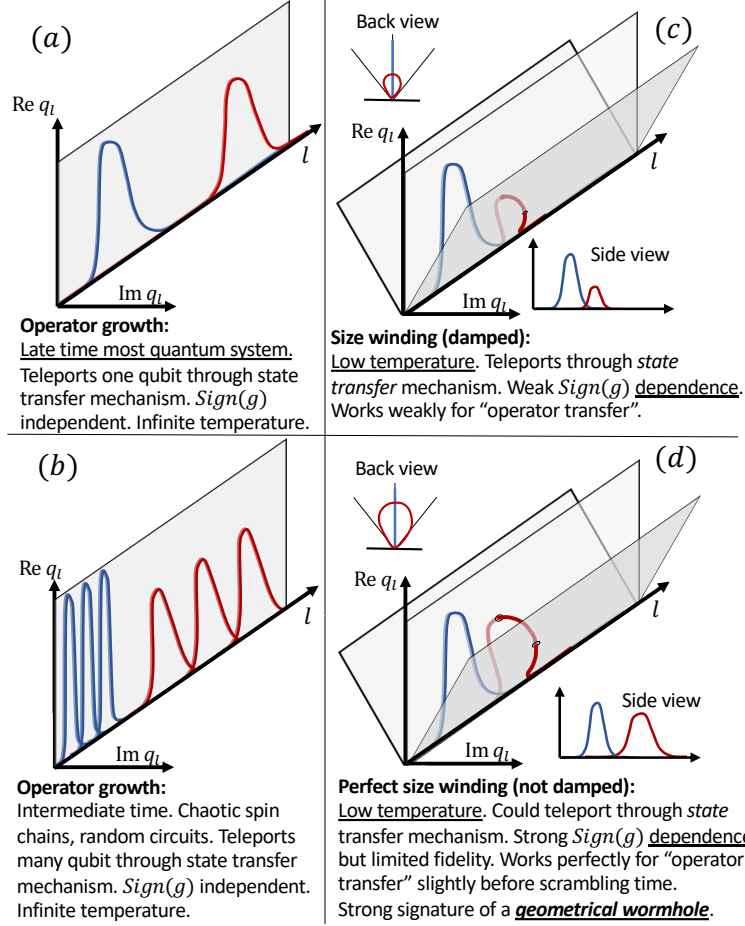


Figure 3. A short summary of paper, discussing different systems, different patterns of operator growth, and consequence of each growth pattern for signal transmission. **Blue:** Initial operator-size distribution. **Red:** Operator-size distribution of the time-evolved operator.

$2^{-n/2} \sum_P c_P P$, where the sum runs over all n -qubit Paulis². Write $|P|$ for the size of an n -qubit Pauli operator, i.e., the number of terms not equal to an identity operator. We define the *winding size distribution*:

$$q(l) := \sum_{|P|=l} c_P^2. \quad (5)$$

The winding size distribution is in contrast to the definition of the conventional size distribution, for which the sum is over the square of the absolute value of c_P . (See [18] for a proper treatment of the conventional definition of size for fermionic systems.) The definitions of the conventional size distribution and the winding size distribution coincide for $\beta = 0$, for which $\rho_\beta^{1/2} O(t)$ is a Hermitian operator and has real expansion coefficients, $c_P \in \mathbb{R}$.

Size winding, in its perfect form, is the following ansatz for the operator wavefunction:

$$\rho_\beta^{1/2} O(t) = \frac{1}{2^{n/2}} \sum_{P \text{ is an } n\text{-qubit Pauli}} e^{i\alpha|P|/n} r_P P, \quad r_P \in \mathbb{R}. \quad (6)$$

² From now on, we suppress the subscripts L and R when there is no confusion.

The key part of this definition is that the coefficients in the size basis acquire an imaginary phase that is linear in the size of the operators.

If we define $|P\rangle_{LR} := P_R |\phi^+\rangle_{LR}$ and assume perfect size winding, then we conclude from the discussion above that

$$O_L^T(-t) |\text{TFD}\rangle = \sum_P e^{i\alpha|P|/n} r_P |P\rangle, \quad (7)$$

$$O_R(t) |\text{TFD}\rangle = \sum_P e^{-i\alpha|P|/n} r_P |P\rangle. \quad (8)$$

Thus, when expressed in the Pauli basis, the difference between the actions of $O_L^T(-t)$ and $O_R(t)$ is given by the “direction” of the winding of the phases of the coefficients.

The role of the coupling e^{igV} on the Pauli basis state $|P\rangle$ is very simple: it gives a phase proportional to $g|P|$ to each $|P\rangle$. In fact, for large $|P|$, a P chosen uniformly at random obeys

$$e^{igV} |P\rangle \simeq e^{-i(4/3)g|P|/n} |P\rangle \quad \text{up to a constant phase.} \quad (9)$$

The discussion above illustrates how the weak coupling can transfer a signal from left to right: with a careful choice of g , the action of the coupling as in Eq. (9) unwinds the distribution in Eq. (7) and winds it in the opposite direction to obtain Eq. (8). This shows that the coupling maps a perturbation of the thermal state of the left system to a perturbation of the right system.

In [13], we will observe that the large- q SYK model exhibits perfect size winding, and at least near-perfect size winding should be present in holographic systems. Indeed, this is to a large extent nothing but a translation of existing results on two point functions for traversable wormholes [2, 18] in the language of size, as we discuss in Sec. III below. We will also see that more general size winding, i.e., a size-dependent phase in $q(l)$ that is not necessarily linear in the size, exists in systems without geometric duals. In fact, even non-local random Hamiltonian evolution can weakly transmit a small amount of information in this fashion.

What we explained above is in the framework of the operator transfer protocol, Figure 1(b), while for the rest of this section we will mostly focus on the state transfer protocol. We will show that state transfer can be done for very generic chaotic quantum systems—even at infinite temperature—and can transmit a small number of qubits with near perfect fidelity.

B. State Transfer by Size-Dependent Phase

In this section, instead of considering the full system $\mathcal{H}_L \otimes \mathcal{H}_R$, we focus on the $2m$ -qubit message system $\mathcal{H}_{A_L} \otimes \mathcal{H}_{A_R}$ (see Fig. 1). The intuition from the operator transfer discussion above will guide the construction here, but the details are different.

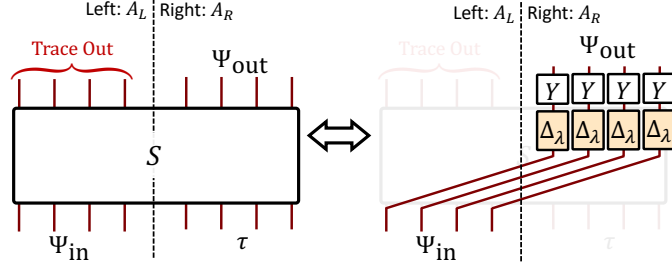
Consider a unitary operator $S = S_{A_L A_R}$ that satisfies

$$S |P\rangle = e^{ig|P|} |P\rangle, \quad \text{for all } m\text{-qubit Paulis } P. \quad (10)$$

This action of S is curiously similar to the action of e^{igV} , but we used a different letter to signify that it is an operator acting on a different Hilbert space. We show in [13] that S maps $\Psi_{\text{in}} \otimes \tau$, with Ψ_{in} an m -qubit initial input state and $\tau \propto I$ the maximally-mixed state, to

$$\Psi_{\text{out}} := \text{Tr}_{A_L} [S(\Psi_{\text{in}} \otimes \tau)] = Y^{\otimes m} \Delta_\lambda^{\otimes m}(\Psi_{\text{in}}) Y^{\otimes m}, \quad (11)$$

after tracing out the left subsystem, where Δ_λ is the single qubit depolarizing channel $\Delta_\lambda(\rho) := (1 - \lambda)\tau + \lambda\rho$, and $\lambda = (1 - \cos(g))/2$. In pictures,



For $g = \pi$ the state transfer is perfect, whereas for $g = 0$ no signal is sent.

Let us return to the wormhole-inspired state transfer protocol at infinite temperature and focus on the full Hilbert space $\mathcal{H}_L \otimes \mathcal{H}_R$. State transfer happens with the aid of the coupling e^{igV} that is acting at $t = 0$. However, the signal is inserted at time $-t$ and probed at time $+t$, hence it is natural to look at the coupling “sandwiched” with time evolutions:

$$\left[e^{+iH_L t} \otimes e^{-iH_R t} \right] e^{igV} \left[e^{-iH_L t} \otimes e^{+iH_R t} \right]. \quad (12)$$

In [13], we argue that in many systems of interest, the net effect of the above sandwiched coupling acting on $\mathcal{H}_L \otimes \mathcal{H}_R$ is nothing but to approximately implement the unitary S (defined in Eq. (10)) on the message subsystem $\mathcal{H}_{A_L} \otimes \mathcal{H}_{A_R}$. In particular, we show that when the evolution is described by a scrambling unitary, the action of the coupling matches Eq. (10) for $m = 1$ (up to a global phase). This demonstrates that the state transfer protocol in that regime can be used to teleport a single qubit. In fact, when the time evolution is modeled by Haar random unitaries, one can rigorously prove that the teleportation channel has low one-shot classical capacity, upper bounded by 3 classical bits.

In [13] we study a variety of systems in detail, including time evolution with totally random Hamiltonians (GUE or GOE ensembles), 2-local Brownian circuits, and spin chains. At very large times all models demonstrate the same behavior, but at intermediate times different systems have different physics.

C. General Bounds on the Fidelity

In this section, we will quote some of the general technical results of [13] for state transfer at arbitrary time and temperature. To be quantitative, we need to use a benchmark for the quality of the channel. Here, we chose the *entanglement fidelity* [22], which we will later refer to as simply the *fidelity* for short. For a quantum channel $\mathcal{C}_{A \rightarrow A}$, entanglement fidelity is the fidelity of the output and input state when the input is a maximally entangled state between A and an environment E of the same dimension: $F := \sqrt{\langle \phi^+ |_{AE} \mathcal{C}_{A \rightarrow A}(\phi^+_{AE}) | \phi^+ \rangle_{AE}}$. Importantly, F lower bounds the average fidelity of the channel over random inputs $|\Psi\rangle_A$. That is, $F \leq \mathbb{E}_{|\Psi\rangle_A} \mathcal{F}(\Psi_A, \mathcal{C}(\Psi_A))$ —see [22].

Assume that Pauli operators with the same initial size l_0 have the same generic operator growth behaviour and denote by q_0 the corresponding winding size distribution (defined as in Eq. (5)). The main player in our bounds is the Fourier transform of the size distribution, which, for $g^2, gm \ll n$, is equal to the left-right two point function:

$$\tilde{q}_{l_0}(g) := \sum_{l=0}^n q_{l_0}(l) e^{-i(4g/3)l/n} \approx e^{-ig} \langle T | O_R(t) e^{igV} O_L^T(-t) | T \rangle \quad (13)$$

The fidelity is a complicated quantity, and it cannot generically be directly evaluated using the size information (or equivalently, two-point function information) alone. However, we can still

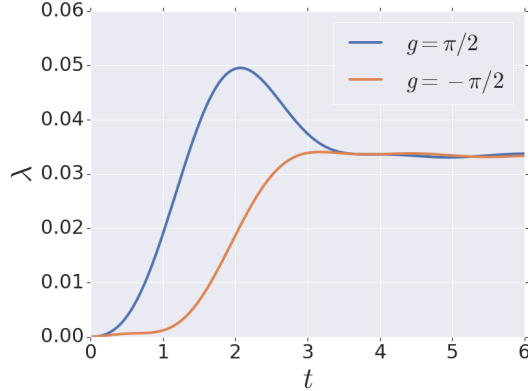


Figure 4. The depolarization parameter λ at infinite n , as a function of time at low temperature ($\beta = 20$) for the averaged state transfer channel using the GOE ensemble of Hamiltonians. The fidelity is improved for positive g at short times, while at large times the sign- g -dependence disappears.

provide strong bounds for fidelity in terms of the simpler quantity F_q , defined to be

$$F_q := \left| \sum_{l=0}^m [N_l/4^m] (-1)^l \tilde{q}_l(g) \right|, \quad (14)$$

where $N_l = \binom{m}{l} 3^l$. One can show that

$$F_q \leq F \leq F_q + \sum_{l=0}^m [N_l/4^m] (1 - |\tilde{q}_l(g)|^2). \quad (15)$$

For local Hamiltonian evolutions, and in a variety of time regimes, F_q can be a good estimate of F as the error term on the right hand side of Eq. (15) will be small.

These relations allow us to rigorously characterize teleportation through various random Hamiltonian and spin chain models, as well as strictly bound the fidelity of different channels even at intermediate times.

As an example, we can see using Eq. (15) why random unitary time evolution at infinite temperature should teleport a single qubit. At $\beta = 0$, q_0 is peaked at $l = 0$ for all times. However, $O(t) = U^\dagger O U$ is a completely random combination of Pauli strings, and its size distribution is peaked at $l = (3/4)n$. Hence, $\tilde{q}_0(g) = 1$, and $\tilde{q}_1(g) \approx e^{-ig}$. Now, $F_q = |3e^{-ig}/4 - 1/4| = \sqrt{1/4 + 3/4(1 - \cos(g))}/2$. Furthermore, since $|q_l| = 1$, Eq. (15) shows that $F_q = F$. Thus, the channel can teleport perfectly when $g = \pi$, as it achieves perfect fidelity.

III. THE HOLOGRAPHIC INTERPRETATION

Figure 2 is very suggestive, and now we will return to the question of whether the geometric picture is a faithful representation of the physics. In other words, when can we claim that a message was sent through an emergent geometry? The teleportation-by-size mechanism we have introduced generalizes the traversable wormhole, and persists even in cases where a fully classical wormhole is not the appropriate description. In fact, we will see that even in the holographic setting, at very large times the teleportation-by-size paradigm remains valid even when the description in terms of a single semi-classical geometry breaks down.

A. Size and momentum

The growth of the size of an operator is a basic manifestation of chaos, and is related to a particle falling towards a black hole horizon [18, 23, 24]. In the context of SYK, or Nearly AdS₂ holography, the bulk interpretation of size is particularly sharp [17], which we now review. In the traversable wormhole, the particle crossing the negative-energy shockwave experiences a (null) translation. The shockwave can therefore be interpreted as the generator of this translation, otherwise known as (null) momentum. The shockwave is a direct consequence of the interaction between the two sides, which in the SYK model is simply the “size” operator. Thus, the size operator is simply related to null momentum [2, 13, 17].

A more precise argument based on [17] can also be given; a detailed version will appear in [13]. Readers unfamiliar with Nearly AdS₂ may jump to the next section. The starting point is that for states close to the thermofield double, the operators defined by

$$B = H_R - H_L, \quad E = H_L + H_R + \mu V - E_0 \quad (16)$$

have a simple geometrical action as a Lorentz boost B , and as global time translation E [25]. Here V is a sum of operators on both sides $V = \sum_{i=1}^k O_i^L O_i^R$; in the SYK model, the simplest choice would be to take $V \propto i \sum \psi_L^j \psi_R^j$ to be the size operator. The value of μ and E_0 should be tuned so that the TFD is an approximate ground state of E , see [25]. It is then natural to consider the combinations

$$P_{\pm} = -\frac{1}{2}(E \pm B). \quad (17)$$

For our purposes, the important point is that $e^{ia^{\pm}P_{\pm}}$ generate a null shift³. By choosing the right sign of a^{\pm} , we can shift the particle backwards so that it traverses the wormhole. Now notice that

$$-P_+ = H_R + \mu V/2, \quad -P_- = H_L + \mu V/2. \quad (18)$$

The remarkable feature of this formula is that the action of P_{\pm} is exceedingly simple on the left/right Hilbert space (equivalently, on one-sided operators), since we can ignore H_L or H_R . For operators on the left (right) side, the amount of P_+ (P_-) momentum inserted is just given by the size, up to some normalization.

This in turn implies that the size wavefunction of a one-sided operator O (e.g., the components of O in a basis of operators organized by size) is dual to the momentum-space wavefunction of the particle created by O . The Fourier transform of the momentum wavefunction is then related to the “position” of the particle in the bulk, where “position” here means the AdS₂ coordinate conjugate to null momentum. Furthermore, the action of the two-sided coupling e^{igV} in the traversable wormhole protocol simply shifts the position of the particle, allowing the particle to potentially exit the black hole.

The upshot is that in a holographic setting, we can clearly see that the winding of the size distribution is related to the location of the particle, e.g., whether the particle is inside or outside of the black hole horizon. The case of imperfect winding can be seen as a generalization of the situation where a good geometric dual exists, though the geometric intuition may still prove useful even in that case.

³ Said more precisely, these generators act as left/right Poincare symmetry generators, which are null shifts at the edge of the Poincare patch.

B. Superpositions of Geometries at Large Times

For times much larger than the scrambling time, the evolution of any chaotic system becomes random. In this regime, a few bits of information can still be transmitted by the coupling. But the interpretation of this signal is not that the particle goes through a semi-classical wormhole, even if the quantum system is in a parameter regime (e.g., large N and strong coupling) where a clean semi-classical description is possible. The reason is the butterfly effect: at large times, a small perturbation (putting in the particle) can destroy any correlations between the two sides that would have existed without the perturbation. The strength of the negative energy shockwave in the bulk is directly proportional to the amount of correlation between the two sides; at very large times, the correlation is simply too weak to shift the particle out of the horizon. Nevertheless, there is another effect [2] involving the interference of two macroscopically different states (or bulk geometries) that allows for information transfer that we will now explain.

Consider the insertion of a message at time $-t$ on the left system using the unitary operator $U_L = e^{i\epsilon\phi_L} \approx 1 + i\epsilon\phi_L$.⁴ At time $t = 0$ we let the left and right systems interact, so that the state is $|\Phi\rangle = e^{igV}U_L(-t)|\text{TFD}\rangle$. We know that the action of e^{igV} depends on the size of the state on which it acts. The key fact is that the operator $\phi_L(-t)$, for large t , is a totally random operator. Therefore, its size is equal to that of a random operator, which is nearly maximal. So e^{igV} acts simply as a relative phase $\theta \sim 1$ between $|\text{TFD}\rangle$ and $\phi_L(-t)|\text{TFD}\rangle$. We can think of it as a phase-shift gate. Then $|\Phi\rangle = |\text{TFD}\rangle + i\epsilon e^{ig\theta}\phi_L(-t)|\text{TFD}\rangle$. This state is a superposition of two vastly different geometries: one is an empty wormhole, given by the state $|\text{TFD}\rangle$, while $\phi_L(-t)|\text{TFD}\rangle$ contains an energetic particle with a significant backreaction on the geometry.

A simple way to record the receipt of the message is to compute the change of the expectation value of $\phi_R(t)$:

$$\langle\Phi|\phi_R(t)|\Phi\rangle - \langle\phi_R(t)\rangle_{\text{therm}} = 2\epsilon \sin(g\theta)\langle\phi_R\phi_L\rangle_{\text{therm}}. \quad (19)$$

See [2, 12] for similar calculations. Clearly, this scenario does not have the interpretation of a classically traversable wormhole. In fact, there is not much geometry left in the description at all. This scenario is contrasted with the situation at shorter times, where we have access to multiple eigenvalues of e^{igV} and the momentum-size correspondence has a clear geometric meaning. In all cases, the dynamics of the phase in the size distribution gives the right description of the physics, but there is a transition from a classical to a quantum picture.

C. Wormhole Tomography and Other Future Directions

There are a number of interesting future directions for investigation. We have focused on two regimes, one relatively short (slightly before the scrambling time) where the particle classically traverses, and the long time effect, which involves interference. This of course does not exhaust the list of non-geometric effects; for example, stringy effects can play an important role at finite coupling, when the string scale is not parametrically suppressed [2]. We have started to explore this in the analytically-tractable playground of the large- q SYK model at finite $\beta\mathcal{J}$ [13].

One might wonder whether it is really possible to operationally distinguish whether the information went “through” the wormhole, or not. We propose the following criteria: if the black hole is in a state where there is a diary behind both horizons, a protocol which involves teleportation “through” the wormhole should be sensitive to what is in the diary. In other words, if Bob claims that he went

⁴ The small- ϵ approximation is not necessary for the conclusions of this section. See [12].

through a wormhole to get to Alice, we can ask him to prove it by giving some description of what was inside the black hole. If we send multiple observers through, they should share information about the interior that is consistent with each other.

In the classically-traversable case, one can imagine therefore engaging in “wormhole tomography,” where the contents of the wormhole interior (as determined by some non-TFD initial state) are probed experimentally by state transfer experiments; the signal exiting the wormhole will be modified in some way by the particular geometry of the wormhole and the presence or absence of any matter.

We analyze size winding in the SYK model in [13], but there are still some open questions about the details of the state transfer protocol in the case where it corresponds to a through-the-wormhole process. Rather than simply swapping a physical qubit with the message qubit, as we have advocated here, one wants to swap the message qubit with a logical qubit that represents, say, the polarization states of an emergent bulk photon. The key fact about this distinction is that the logical subspace for the encoding has fixed bulk energy, so the gravitational backreaction does not depend on the message. This is one way to avoid superpositions of macroscopically different geometries. There is no obstruction preventing us from carrying out this task in principle, and it might be instructive to actually do it. The problem is one of engineering, and a more complicated model like $\mathcal{N} = 4$ super Yang-Mills theory might be required in order to have the necessary ingredients.

IV. EXPERIMENTAL REALIZATION

As discussed above, this work concerns a whole family of protocols, all of which are interesting to study experimentally for the light they would shed on entanglement, chaos, and holography. For example, if the system under study has a simple dual holographic description, such as the SYK model [26–33] or certain supersymmetric gauge theories, the experiments described here can directly probe traversable wormholes. More generally, these experiments probe communication phenomena inspired by and related to the traversable wormhole phenomenon in holographic models. The key ingredients are as follows.

First, one must be able to prepare a thermofield double state associated with H . This means preparing a special entangled state of two copies of the physical system, the left and right systems. At infinite temperature, the thermofield double state is just a collection of Bell pairs between left and right (or the appropriate fermionic version). For general Hamiltonians and non-infinite temperature, there is no known procedure to prepare the thermofield double state. However, there are recently proposed approximate methods that are applicable to systems of interest including the SYK model and various spin chains [34–36].

Second, one must be able to effectively evolve forward and backward in time with the system Hamiltonian H . More precisely, we require the ability to evolve forward and backward with $H_L = H$ on the left system and the ability to evolve forward with the CPT conjugate of H , $H_R = H^T$, on the right system. Given a fully controlled fault-tolerant quantum computer and a Trotterized approximation of e^{-iHt} , it is in principle no more challenging to implement e^{+iHt} (backward evolution) than it is to implement e^{-iHt} (forward evolution). However, to implement forward and backward time evolution in a specialized quantum simulator requires specific capabilities. In the context of measurements of out-of-time-order correlators, various techniques have been developed to achieve this level of control, at least approximately [37–46].

Third, one must be able to apply the weak left-right coupling given by the V operator. More precisely, it must be possible to generate the unitary e^{igV} . This coupling must be applied suddenly, in between the other time-evolution segments of the circuit.

Fourth, one must be able to apply local control operations, including deleting and inserting qubits, performing local unitary operations, and making local measurements in a general basis. This requires some degree of individual qubit addressability, although in the simplest cases one only needs to single out a small number of qubits.

Given these capabilities, the general protocols in Fig. 1 can be carried out. For concreteness, the remainder of this section will focus on the case of the insertion/deletion protocol, Fig. 1(a). To give an example, consider the deletion/insertion protocol at infinite temperature when $g = \pi$, all times involved are large, n is very large, and $m = 1$. In this case, $\Psi_{\text{out}} = Y\Psi_{\text{in}}Y$ with perfect fidelity.

A. Rydberg atom arrays

One platform where such phenomena could be studied is Rydberg atom arrays. In one implementation [47], information is encoded in a pair of levels in ^{87}Rb , a ground state $|g\rangle$ and a Rydberg state $|r\rangle$, such that the effective Hamiltonian can be written in a spin-chain form as

$$H = \sum_i \frac{\Omega_i}{2} X_i + \sum_i \Delta_i \frac{I - Z_i}{2} + \frac{1}{4} \sum_{i < j} V_{ij} (I - Z_i)(I - Z_j), \quad (20)$$

where $Z_i = |g_i\rangle\langle g_i| - |r_i\rangle\langle r_i|$ and $X_i = |g_i\rangle\langle r_i| + |r_i\rangle\langle g_i|$, Ω_i and Δ_i are tunable field parameters, and V_{ij} is the van der Waals interaction between the atoms.

In terms of capabilities listed above, preparation of an infinite-temperature thermofield double state (i.e., Bell pairs) has already been achieved using Rydberg atoms [48]. For finite temperatures, the approximate methods discussed above could also be applied to this setup. One can engineer the requisite backwards time evolution in various ways. One possibility is to work in the blockade regime, in which the effective dynamics takes place in a constrained Hilbert space and is governed just by the fields Ω and Δ . These parameters can be reversed with echo pulse sequences and so forward and backward evolution is possible. Below we will also discuss a different Floquet scheme. The left/right coupling $V = \frac{1}{n-m} \sum_i Z_i^L Z_i^R$ is also feasible in a Rydberg system, and is already needed to prepare the Bell states. Finally, local addressing is possible and localized readout has been demonstrated [47].

One particularly interesting system to consider is a Floquet version of the Rydberg Hamiltonian known as the kicked quantum Ising model. Although experiments here are naturally restricted to infinite temperature because of heating, the driving is interesting because it can enhance chaos and aid in the problem of backward and forward time evolution. Consider, for example, the kicked quantum Ising model of Prosen et al. [49], in which the time evolution for one time step is given by

$$U = U_K U_I \quad (21)$$

where

$$U_K = \exp\left(ib \sum_i X_i\right) \quad (22)$$

and

$$U_I = \exp\left(iJ \sum_i Z_i Z_{i+1} + i \sum_i h_i Z_i\right). \quad (23)$$

The parameters of the model are J , b , and the set of local fields h_i . Remarkably, if $J = b = \pi/4$ and h_i are drawn uniformly at random from a Gaussian distribution with variance σ , then the model

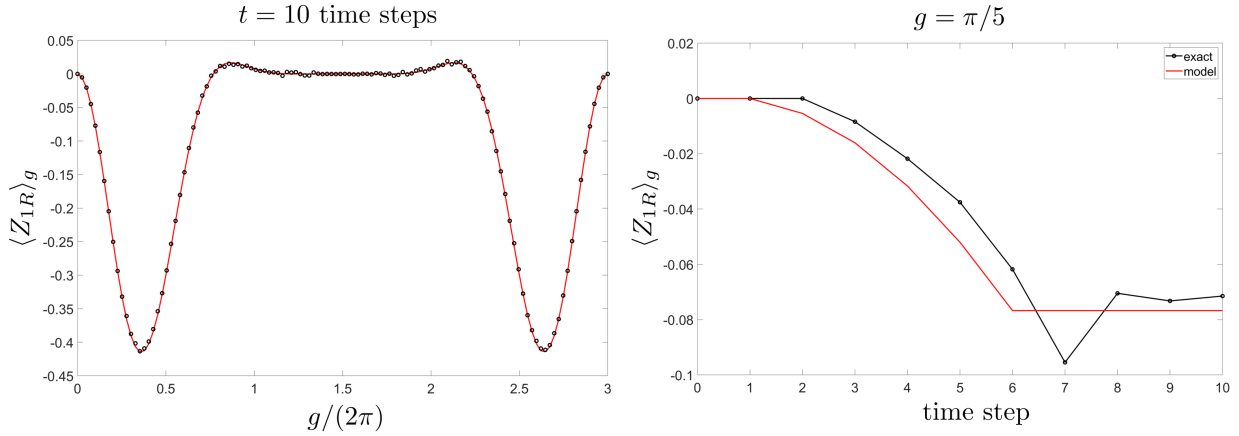


Figure 5. Expectation value of Z_{1R} after injection of $Z_{1L} = 1$ state on the left system. Black dots are direct numerical simulation of the protocol in the quantum kicked Ising model with $n = 7$ spins on the left and right and with $J = b = \pi/4$ and h_i drawn from a box distribution of width .5. **Left:** Signal at fixed large time as a function of g . The black circles are the exact numerical simulation. The red curve is the theory prediction in Eq. (24). **Right:** Signal at fixed g as a function of time step. The black circles are the exact numerical simulation. The red curve is a crude approximation where we assume Eq. (24) holds at all times with the effective system size replaced as $n \rightarrow \min(t + 1, n)$.

is in a sense maximally chaotic (albeit not in the out-of-time-order correlator sense). For example, the entanglement entropy of subsystems grows as rapidly as possible when starting from a product state [49]. We note that a hyperfine encoding for qubits (instead of directly using the Rydberg level) might be useful for this kind of gate-like time dynamics [50].

This kicked model is particularly appealing because the infinite-temperature thermofield double state is easier to prepare and because it allows easier control over the evolution. This relative ease is due to the fact that the spectra of $\sum_i X_i$ and $\sum_i Z_i Z_{i+1}$ are integer, so that one has, for example, $U_K(b+2\pi) = U_K(b)$. Thus, backward evolution corresponds to $U_K(b)^{-1} = U_K(-b) = U_K(2\pi - b)$, so one can achieve backward time evolution by over-evolving in the forward direction. This covers the transverse field and interaction terms; the longitudinal field terms can be dealt with using a standard echo sequence. One important point is that if the left evolution for one time step is U , then the right evolution for one time step must be $U^T = U_I U_K$ (note the reverse ordering of the pulsed terms, which are individually symmetric).

In Fig. 5, we show an exact numerical simulation of the experimental protocol for $n = 7$ atoms on the left and right. We inject a pure state with eigenvalue $Z_{1L} = 1$ into the first qubit on the left. Then, as a more experimentally accessible stand-in for the full fidelity, we show the result of measuring the expectation value of Z_{1R} on the right. The black dots are the exact simulation and the red curves are obtained from our theory calculations. In particular, for a system with n atoms and left-right coupling g at large time, the prediction for the expectation value is

$$\langle Z_{1R} \rangle_g = \left(\cos \frac{g}{n-1} \right)^{n-1} \frac{-\left(\cos \frac{g}{n-1} \right)^{n-1} + \cos g}{2}. \quad (24)$$

As can be seen from the left panel of Fig. 5, the theory prediction perfectly fits the exact simulation data in the kicked quantum Ising model.

B. Trapped ions

While the Rydberg atom arrays just discussed have a natural spatial structure to their interactions, it is also quite interesting to consider systems which can support few-body but geometrically non-local interactions. One such system is an ion trap quantum processor, e.g. [51]. By driving vibrational modes of an ionic crystal, one can engineer a rich pattern of all-to-all interactions [52]. Such systems are interesting because they mimic the structure of the SYK model and other matrix models that exhibit low-energy dynamics governed by a simple gravitational effective theory. One can again consider analog or digital versions of the platform, and in the digital case all the needed capabilities are present. Particularly interesting is a recent small-scale preparation of approximate thermofield double states on such a digital ion trap quantum processor [53].

C. Closing remarks

We have discussed two candidate systems, but many other platforms should be able to realize the physics discussed here. In [13] we study a wide variety of models, including spin chains, random circuits, random Hamiltonians, and the SYK model, and some of these would be more naturally suited to other platforms, for example, proposals to realized SYK in simulators [54, 55] or on digital devices [56, 57]

In closing, let us highlight some of the conceptual and practical issues that will be faced in any experimental effort along the lines we discuss here. On the practical side, one key question is the impact of noise and experimental imperfections on our protocols, especially imperfect time-reversal due to over- or under-evolution and effects of environmental decoherence. Preliminary simulations indicate that the basic physics can still be seen when imperfections are below the 5% level for modest system size and time, but much more study is needed in the context of particular platforms. This general class of observables does exhibit some forms of resilience [58]. Another crucial question is how well the thermofield double state must be prepared to see the physics we discuss.

On the conceptual side, we must ask what we ultimately hope to learn about nature from such experiments. We emphasized above that the infinite-temperature large-time example does not correspond to geometrical motion through a semi-classical wormhole. For one thing, only a single qubit can be teleported with high fidelity in the high-temperature limit, but with the right encoding of information many qubits can be sent at low temperature and intermediate time in a holographic system hosting a traversable wormhole. Instead, the infinite-temperature example probes a physical effect common to all chaotic quantum systems with many degrees of freedom, including quantum gravitational systems.

From these considerations, it should be clear that measuring a successful teleportation signal for a single qubit is not enough to guarantee a semi-classical traversable wormhole in the bulk. One needs additional conditions that can be tested within the framework discussed here by varying the time t , the coupling g , and the way input information is encoded. Hence, while one long-term goal of such experiments is to detect and study wormholes arising holographically in highly entangled systems, there are other goals. More generally, the purpose is to shed light on deep and theoretically challenging questions about nature, including the necessary conditions to have a semi-classical bulk and the effects of quantum and stringy corrections to the semi-classical gravity picture. Thus, we believe the experiments described here are worth the effort to realize the long-term potential for experimental insight into quantum gravity.

Acknowledgements.— We thank Patrick Hayden, Misha Lukin, Chris Monroe, Geoff Penington, John Preskill, Xiaoliang Qi, Douglas Stanford, Alexandre Streicher, and Zhenbin Yang for fruitful

discussions. We also thank Iris Cong, Emil Khabiboulline, Harry Levine, Misha Lukin, Hannes Pichler, and Cris Zanolini for collaboration on related work. H.G. is supported by the Simons Foundation through It from Qubit collaboration. H.L. is supported by an NDSEG fellowship. G.S. is supported by DOE award Quantum Error Correction and Spacetime Geometry DE-SC0018407, the Simons Foundation via It From Qubit, and the IQIM at Caltech (NSF Grant PHY-1733907). L.S. is supported by NSF Award Number 1316699. B.S. acknowledges support from the Simons Foundation via It From Qubit and from the Department of Energy via the GeoFlow consortium. M.W. is supported by an NWO Veni grant no. 680-47-459.

-
- [1] Ping Gao, Daniel Louis Jafferis, and Aron C. Wall, “Traversable wormholes via a double trace deformation,” *Journal of High Energy Physics* **2017**, 151 (2017).
 - [2] Juan Maldacena, Douglas Stanford, and Zhenbin Yang, “Diving into traversable wormholes,” *Fortschritte der Physik* **65**, 1700034 (2017).
 - [3] Gerard ’t Hooft, “Dimensional reduction in quantum gravity,” *Conference on Highlights of Particle and Condensed Matter Physics (SALAMFEST) Trieste, Italy, March 8-12, 1993*, Conf. Proc. **C930308**, 284–296 (1993), arXiv:gr-qc/9310026 [gr-qc].
 - [4] Leonard Susskind, “The World as a Hologram,” *J. Math. Phys.* **36**, 6377–6396 (1995), arXiv:hep-th/9409089 [hep-th].
 - [5] Juan Martin Maldacena, “The Large N limit of superconformal field theories and supergravity,” *Int. J. Theor. Phys.* **38**, 1113–1133 (1999), [Adv. Theor. Math. Phys.2,231(1998)], arXiv:hep-th/9711200 [hep-th].
 - [6] S.S. Gubser, I.R. Klebanov, and A.M. Polyakov, “Gauge theory correlators from non-critical string theory,” *Physics Letters B* **428**, 105–114 (1998).
 - [7] Edward Witten, “Anti de sitter space and holography,” (1998), arXiv:hep-th/9802150 [hep-th].
 - [8] Tom Banks, W. Fischler, S. H. Shenker, and Leonard Susskind, “M theory as a matrix model: A Conjecture,” *Phys. Rev. D* **55**, 5112–5128 (1997), [435(1996)], arXiv:hep-th/9610043 [hep-th].
 - [9] Yasuhiro Sekino and L Susskind, “Fast scramblers,” *Journal of High Energy Physics* **2008**, 065–065 (2008).
 - [10] Patrick Hayden and John Preskill, “Black holes as mirrors: Quantum information in random subsystems,” *JHEP* **09**, 120 (2007), arXiv:0708.4025 [hep-th].
 - [11] Charles H. Bennett, Gilles Brassard, Claude Crepeau, Richard Jozsa, Asher Peres, and William K. Wootters, “Teleporting an unknown quantum state via dual classical and Einstein-Podolsky-Rosen channels,” *Phys. Rev. Lett.* **70**, 1895–1899 (1993).
 - [12] Ping Gao and Hong Liu, “Regenesis and quantum traversable wormholes,” arXiv preprint (2018), arXiv:1810.01444.
 - [13] Sepehr Nezami, Adam R. Brown, Hrant Gharibyan, Stefan Leichenauer, Henry W. Lin, Grant Salton, Leonard Susskind, Brian Swingle, and Michael Walter, “Teleportation by size,” to appear.
 - [14] Ben Freivogel, Damián A. Galante, Dora Nikolakopoulou, and Antonio Rotundo, “Traversable wormholes in ads and bounds on information transfer,” (2019), arXiv:1907.13140 [hep-th].
 - [15] Beni Yoshida and Alexei Kitaev, “Efficient decoding for the Hayden-Preskill protocol,” arXiv:1710.03363 (2017).
 - [16] Leonard Susskind, “Complexity and Newton’s Laws,” arXiv preprint (2019), arXiv:1904.12819.
 - [17] Henry W Lin, Juan Maldacena, and Ying Zhao, “Symmetries near the horizon,” arXiv preprint (2019), arXiv:1904.12820.

- [18] Xiao-Liang Qi and Alexandre Streicher, “Quantum epidemiology: operator growth, thermal effects, and SYK,” *Journal of High Energy Physics* **2019**, 12 (2019).
- [19] Adam Nahum, Sagar Vijay, and Jeongwan Haah, “Operator spreading in random unitary circuits,” *Physical Review X* **8** (2018), 10.1103/physrevx.8.021014.
- [20] C. W. von Keyserlingk, Tibor Rakovszky, Frank Pollmann, and S. L. Sondhi, “Operator hydrodynamics, otocs, and entanglement growth in systems without conservation laws,” *Physical Review X* **8** (2018), 10.1103/physrevx.8.021013.
- [21] Shenglong Xu and Brian Swingle, “Locality, quantum fluctuations, and scrambling,” *Physical Review X* **9** (2019), 10.1103/physrevx.9.031048.
- [22] Benjamin Schumacher, “Sending entanglement through noisy quantum channels,” *Physical Review A* **54**, 2614 (1996).
- [23] Daniel A. Roberts, Douglas Stanford, and Alexandre Streicher, “Operator growth in the SYK model,” *JHEP* **06**, 122 (2018), arXiv:1802.02633 [hep-th].
- [24] Adam R. Brown, Hrant Gharibyan, Alexandre Streicher, Leonard Susskind, Larus Thorlacius, and Ying Zhao, “Falling Toward Charged Black Holes,” *Phys. Rev.* **D98**, 126016 (2018), arXiv:1804.04156 [hep-th].
- [25] Juan Maldacena and Xiao-Liang Qi, “Eternal traversable wormhole,” arXiv preprint (2018), arXiv:1804.00491.
- [26] Subir Sachdev and Jinwu Ye, “Gapless spin-fluid ground state in a random quantum heisenberg magnet,” *Phys. Rev. Lett.* **70**, 3339–3342 (1993).
- [27] Antoine Georges, Olivier Parcollet, and Subir Sachdev, “Mean field theory of a quantum heisenberg spin glass,” *Phys. Rev. Lett.* **85**, 840–843 (2000).
- [28] A. Georges, O. Parcollet, and S. Sachdev, “Quantum fluctuations of a nearly critical heisenberg spin glass,” *Phys. Rev. B* **63**, 134406 (2001).
- [29] Alexei Kitaev, “A simple model of quantum holography.” (Talks at KITP, April 7, 2015 and May 27, 2015.), <http://online.kitp.ucsb.edu/online/entangled15/kitaev/>, <http://online.kitp.ucsb.edu/online/entangled15/kitaev2/>.
- [30] Joseph Polchinski and Vladimir Rosenhaus, “The spectrum in the sachdev-ye-kitaev model,” *Journal of High Energy Physics* **2016**, 1–25 (2016).
- [31] Juan Maldacena and Douglas Stanford, “Remarks on the Sachdev-Ye-Kitaev model,” *Phys. Rev.* **D94**, 106002 (2016), arXiv:1604.07818 [hep-th].
- [32] Dmitry Bagrets, Alexander Altland, and Alex Kamenev, “Power-law out of time order correlation functions in the SYK model,” *Nucl. Phys.* **B921**, 727–752 (2017), arXiv:1702.08902 [cond-mat.str-el].
- [33] Antonio M. García-García and Jacobus J. M. Verbaarschot, “Spectral and thermodynamic properties of the sachdev-ye-kitaev model,” *Physical Review D* **94** (2016), 10.1103/physrevd.94.126010.
- [34] John Martyn and Brian Swingle, “Product spectrum ansatz and the simplicity of thermal states,” *Physical Review A* **100** (2019), 10.1103/physreva.100.032107.
- [35] William Cottrell, Ben Freivogel, Diego M. Hofman, and Sagar F. Lokhande, “How to build the thermofield double state,” *Journal of High Energy Physics* **2019** (2019), 10.1007/jhep02(2019)058.
- [36] Jingxiang Wu and Timothy H. Hsieh, “Variational thermal quantum simulation via thermofield double states,” (2018), arXiv:1811.11756 [cond-mat.str-el].
- [37] Brian Swingle, Gregory Bentsen, Monika Schleier-Smith, and Patrick Hayden, “Measuring the scrambling of quantum information,” *Phys. Rev.* **A94**, 040302 (2016), arXiv:1602.06271 [quant-ph].
- [38] Norman Y. Yao, Fabian Grusdt, Brian Swingle, Mikhail D. Lukin, Dan M. Stamper-Kurn, Joel E. Moore, and Eugene A. Demler, “Interferometric Approach to Probing Fast Scrambling,” arXiv:1607.01801 (2016).

- [39] Guanyu Zhu, Mohammad Hafezi, and Tarun Grover, “Measurement of many-body chaos using a quantum clock,” *Phys. Rev. A* **94**, 062329 (2016).
- [40] Michele Campisi and John Goold, “Thermodynamics of quantum information scrambling,” *Phys. Rev. E* **95**, 062127 (2017).
- [41] Nicole Yunger Halpern, “Jarzynski-like equality for the out-of-time-ordered correlator,” *Phys. Rev. A* **95**, 012120 (2017).
- [42] Beni Yoshida and Norman Y Yao, “Disentangling Scrambling and Decoherence via Quantum Teleportation,” *Phys. Rev. X* **9**, 011006 (2019).
- [43] Jun Li, Ruihua Fan, Hengyan Wang, Bingtian Ye, Bei Zeng, Hui Zhai, Xinhua Peng, and Jiangfeng Du, “Measuring out-of-time-order correlators on a nuclear magnetic resonance quantum simulator,” *Phys. Rev. X* **7**, 031011 (2017).
- [44] Martin Garttner, Justin G. Bohnet, Arghavan Safavi-Naini, Michael L. Wall, John J. Bollinger, and Ana Maria Rey, “Measuring out-of-time-order correlations and multiple quantum spectra in a trapped-ion quantum magnet,” *Nat. Phys.* **13**, 781–786 (2017).
- [45] Eric J. Meier, Jackson Ang’ong’a, Fangzhao Alex An, and Bryce Gadway, “Exploring quantum signatures of chaos on a Floquet synthetic lattice,” *Phys. Rev. A* **100**, 013623 (2019).
- [46] K. A. Landsman, C. Figgatt, T. Schuster, N. M. Linke, B. Yoshida, N. Y. Yao, and C. Monroe, “Verified quantum information scrambling,” *Nature* **567**, 61–65 (2019).
- [47] Hannes Bernien, Sylvain Schwartz, Alexander Keesling, Harry Levine, Ahmed Omran, Hannes Pichler, Soonwon Choi, Alexander S. Zibrov, Manuel Endres, Markus Greiner, Vladan Vuletić, and Mikhail D. Lukin, “Probing many-body dynamics on a 51-atom quantum simulator,” *Nature* **551**, 579–584 (2017).
- [48] Harry Levine, Alexander Keesling, Giulia Semeghini, Ahmed Omran, Tout T. Wang, Sepehr Ebadi, Hannes Bernien, Markus Greiner, Vladan Vuletić, Hannes Pichler, and Mikhail D. Lukin, “Parallel implementation of high-fidelity multiqubit gates with neutral atoms,” *Phys. Rev. Lett.* **123**, 170503 (2019).
- [49] Bruno Bertini, Pavel Kos, and Tomaž Prosen, “Entanglement spreading in a minimal model of maximal many-body quantum chaos,” *Physical Review X* **9** (2019), 10.1103/physrevx.9.021033.
- [50] Harry Levine, Alexander Keesling, Giulia Semeghini, Ahmed Omran, Tout T. Wang, Sepehr Ebadi, Hannes Bernien, Markus Greiner, Vladan Vuletić, Hannes Pichler, and Mikhail D. Lukin, “Parallel implementation of high-fidelity multiqubit gates with neutral atoms,” *Physical Review Letters* **123** (2019), 10.1103/physrevlett.123.170503.
- [51] K. Wright, K. M. Beck, S. Debnath, J. M. Amini, Y. Nam, N. Grzesiak, J. S. Chen, N. C. Pimenti, M. Chmielewski, C. Collins, K. M. Hudek, J. Mizrahi, J. D. Wong-Campos, S. Allen, J. Apisdorf, P. Solomon, M. Williams, A. M. Ducore, A. Blinov, S. M. Kreikemeier, V. Chaplin, M. Keesan, C. Monroe, and J. Kim, “Benchmarking an 11-qubit quantum computer,” (2019), arXiv:1903.08181 [quant-ph].
- [52] Zohreh Davoudi, Mohammad Hafezi, Christopher Monroe, Guido Pagano, Alireza Seif, and Andrew Shaw, “Towards analog quantum simulations of lattice gauge theories with trapped ions,” (2019), arXiv:1908.03210 [quant-ph].
- [53] D. Zhu, S. Johri, N. M. Linke, K. A. Landsman, N. H. Nguyen, C. H. Alderete, A. Y. Matsuura, T. H. Hsieh, and C. Monroe, “Variational generation of thermofield double states and critical ground states with a quantum computer,” (2019), arXiv:1906.02699 [quant-ph].
- [54] Ipei Danshita, Masanori Hanada, and Masaki Tezuka, “Creating and probing the Sachdev-Ye-Kitaev model with ultracold gases: Towards experimental studies of quantum gravity,” *Progress of Theoretical and Experimental Physics* **2017** (2017), 10.1093/ptep/ptx108.
- [55] D. I. Pikulin and M. Franz, “Black hole on a chip: Proposal for a physical realization of the Sachdev-

- Ye-Kitaev model in a solid-state system,” *Physical Review X* **7** (2017), 10.1103/physrevx.7.031006.
- [56] L. García-Álvarez, I. L. Egusquiza, L. Lamata, A. del Campo, J. Sonner, and E. Solano, “Digital quantum simulation of minimal ads/cft,” *Physical Review Letters* **119** (2017), 10.1103/physrevlett.119.040501.
- [57] Ryan Babbush, Dominic W. Berry, and Hartmut Neven, “Quantum simulation of the Sachdev-Ye-Kitaev model by asymmetric qubitization,” *Physical Review A* **99** (2019), 10.1103/physreva.99.040301.
- [58] Brian Swingle and Nicole Yunger Halpern, “Resilience of scrambling measurements,” *Physical Review A* **97** (2018), 10.1103/physreva.97.062113.